

Evolution of the latitudinal diversity gradient in the hyperdiverse ant genus *Pheidole*

Evan P. Economo^{1,2*}, Jen-Pan Huang², Georg Fischer¹, Eli M. Sarnat¹, Nitish Narula¹, Milan Janda^{3,4}, Benoit Guénard⁵, John T. Longino⁶, L. Lacey Knowles²

*correspondence: Evan P. Economo, evaneconomo@gmail.com

¹*Okinawa Institute of Science and Technology Graduate University, Onna, Okinawa, Japan, 904-0495*

²*Department of Ecology & Evolutionary Biology, Museum of Zoology, University of Michigan, USA*

³*National Laboratory for Ecological Analysis and Synthesis (LANASE), ENES, UNAM, Morelia, Mexico*

⁴*Biology Centre of Czech Academy of Sciences, Ceske Budejovice, Czech Republic*

⁵*The University of Hong Kong, School of Biological Sciences, Hong Kong, SAR, China.*

⁶*Department of Biology, University of Utah, USA*

Acknowledgements: This work was supported by NSF (DEB-1145989 to EPE and LLK), by subsidy funding to OIST, and by a Japan Society for the Promotion of Science Kakenhi (17K15180) to EPE. We thank P.S. Ward and B.L. Fisher for sharing specimens and for all the data contributors to the GABI project.

Biosketch: The research team is interested in the ecology and evolution of biodiversity, **This is the author manuscript accepted for publication and has undergone full peer review but has not been through the copyediting, typesetting, pagination and proofreading process, which may lead to differences between this version and the [Version of Record](#). Please cite this article as [doi: 10.1111/geb.12867](https://doi.org/10.1111/geb.12867)**

This article is protected by copyright. All rights reserved

especially insects.

Author Manuscript

1
2
3
4
5
6
7
8
9
10
11
12
13
14
15
16
17
18
19
20
21
22
23
24
25
26
27
28
29
30
31
32

PROFESSOR EVAN ECONOMO (Orcid ID : 0000-0001-7402-0432)

DR. BENOIT GUENARD (Orcid ID : 0000-0002-7144-1175)

DR. JOHN T. LONGINO (Orcid ID : 0000-0001-5465-0293)

Article type : Research Papers

Evolution of the latitudinal diversity gradient in the hyperdiverse ant genus *Pheidole*

Running title: Evolution of tropical hyperdiversity in ants

Evan P. Economo^{1,2*}, Jen-Pan Huang², Georg Fischer¹, Eli M. Sarnat¹, Nitish Narula¹, Milan Janda^{3,4}, Benoit Guénard⁵, John T. Longino⁶, L. Lacey Knowles²

*correspondence: Evan P. Economo, evaneconomo@gmail.com

¹Okinawa Institute of Science and Technology Graduate University, Onna, Okinawa, Japan, 904-0495

²Department of Ecology & Evolutionary Biology, Museum of Zoology, University of Michigan, USA

³National Laboratory for Ecological Analysis and Synthesis (LANASE), ENES, UNAM, Morelia, Mexico

⁴Biology Centre of Czech Academy of Sciences, Ceske Budejovice, Czech Republic

⁵The University of Hong Kong, School of Biological Sciences, Hong Kong, SAR, China.

⁶Department of Biology, University of Utah, USA

33 **ABSTRACT**

34

35 **Aim**

36 The latitudinal diversity gradient is the dominant pattern of life on Earth, but a consensus
37 understanding of its origins has remained elusive. The analysis of recently diverged, hyper-
38 rich invertebrate groups provides an opportunity to investigate latitudinal patterns with the
39 statistical power of large trees while minimizing potentially confounding variation in ecology
40 and history. Here, we synthesize global phylogenetic and macroecological data on a
41 hyperdiverse (>1100 species) ant radiation, Pheidole, and test predictions of three general
42 explanations for the latitudinal gradient: variation in diversification rates, tropical
43 conservatism, and ecological regulation.

44

45 **Location**

46 Global.

47

48 **Time Period**

49 The past 35 million years.

50

51 **Major taxa studied**

52 The hyperdiverse ant genus Pheidole Westwood.

53

54 **Methods**

55 We assembled geographic data for 1499 species and morphospecies, and inferred a dated
56 phylogeny for 449 species of the Pheidole, including 167 species newly sequenced for this
57 study. We tested for correlations between diversification rate and latitude with BAMM,
58 HiSSE, GeoSSE, and FiSSE, evaluated evidence for richness steady state, and examined
59 patterns of diversification as Pheidole spread around the globe.

60

61 **Results**

62 There was no evidence of systematic variation of net diversification rates with latitude across
63 any of the methods. We found that Pheidole diversification occurred in bursts when new
64 continents were colonized, followed by a slowdown in each region, but there is no evidence
65 richness has saturated at an equilibrium in any region. Additionally, we found latitudinal

66 affinity is moderately conserved with a Neotropical ancestor and simulations show that
67 phylogenetic inertia alone is sufficient to produce the gradient pattern.

68

69 **Main Conclusions**

70 Our results provide no evidence that diversification rates vary systematically with latitude.
71 Richness is far from steady state in each region, contrary to the ecological regulation
72 hypothesis, although there is evidence that ecological opportunity promotes diversification
73 after colonization of new areas. The fact that niche conservatism is strong enough to produce
74 the gradient pattern is in accord with the tropical conservatism hypothesis. Overall, these
75 results shed light on the mechanisms underlying the emergence of the diversity gradient
76 within the past 34 million years, complementing recent work on deeper timescales, and more
77 generally contribute toward a much-needed invertebrate perspective on global biodiversity
78 dynamics.

79

80 **Keywords:** ants, latitudinal diversity gradient, tropical conservatism, diversification rate,
81 diversity regulation, macroevolution

82

83

84

85

86 **INTRODUCTION**

87

88 Understanding how ecological and evolutionary processes interact with historical
89 factors to shape global biodiversity patterns remains a major goal of biology. The latitudinal
90 diversity gradient (LDG) is the most general biogeographic pattern, yet we still lack a
91 consensus understanding of its mechanisms (Pianka, 1966; Willig et al., 2003; Mittelbach et
92 al., 2007; Fine, 2015). This is likely because many biological, physical, and historical factors
93 that could plausibly affect diversity vary systematically with latitude, and thus a large number
94 of hypotheses have been developed to explain the pattern. However, testing the predictions of
95 different hypotheses empirically and evaluating their relative merits has proven to be a
96 challenge.

97

98 Recently, the synthesis of large-scale geographic datasets along with large-scale
phylogenetic data has provided new opportunities for empirical evaluation of hypotheses for

99 the mechanisms underlying the LDG. These tests have mainly focused on vertebrates (e.g.
100 Cardillo et al., 2005; Weir & Schluter, 2007; Jetz et al., 2012; Pyron & Wiens, 2013; Rolland
101 et al., 2014; Duchêne & Cardillo, 2015; Siqueira et al. 2016; Pigot et al., 2016) and woody
102 plants (Kerkhoff et al., 2014), since those are the taxa with large-scale comprehensive data
103 available. Several pioneering studies have examined latitudinal diversification patterns in
104 insects (e.g. McKenna & Farrell, 2006; Hawkins & DeVries, 2009; Condamine et al., 2012;
105 Moreau & Bell, 2013; Pie, 2016; Owens et al., 2017), although data-deficiency of most
106 invertebrate groups makes taxonomic and/or geographic scope a challenge for analysis.

107 Among invertebrates, ants are emerging as an exemplar taxon for global biodiversity
108 studies. Ants are ecologically dominant in most terrestrial ecosystems and are, for an insect
109 group, relatively well documented scientifically. Moreover, their diversity is high, but not
110 intractably so, with richness on the same order as major vertebrate groups (~15,000 described
111 ant species), and ants exhibit a marked latitudinal diversity gradient (Kaspari et al., 2004;
112 Dunn et al., 2009). Recently, a new comprehensive dataset has been compiled which gives
113 the known geographic distribution of all described ant species across >400 geographic
114 regions around the globe (Guénard et al., 2017). These data, combined with progress toward
115 reconstructing the ant tree of life (Brady et al., 2006; Moreau et al., 2006; Moreau & Bell,
116 2013; Ward et al., 2015), allow for inferences of the evolutionary underpinnings of large-
117 scale diversity patterns in ants.

118 Here, we use the globally distributed, hyperdiverse (>1100 described species) ant
119 genus *Pheidole* as a model taxon to test hypotheses for the latitudinal diversity gradient.
120 While over a hundred hypotheses have been proposed to explain the gradient (Willig et al.,
121 2003; Mittelbach et al., 2007; Fine, 2015), these can be placed under three umbrella
122 hypotheses: i) the Diversification Rate hypothesis (DRH), ii) the Tropical Conservatism
123 Hypothesis (TCH), and iii) the Ecological Regulation Hypothesis (ERH).

124 The Diversification Rate Hypothesis posits that there is some causal factor that affects
125 speciation and/or extinction rates and varies with latitude (e.g. reviewed in Pianka, 1966;
126 Mittelbach et al., 2007; Fine, 2015). This leads to a latitudinal disparity in species
127 accumulation rate that underlies the gradient, rather than any regulation of total species
128 numbers. Many such potential causal factors have been proposed. For example, temperature
129 may affect mutation rates, which in turn could affect the rates of evolution of reproductive
130 incompatibilities (Rohde, 1992). Or, extinction rates could be higher in the temperate than
131 tropical zone due greater climatic variability (Weir & Schluter, 2007; Rolland et al., 2014).

132 The prediction of the DRH is straightforward: net diversification rate inferred from a
133 phylogeny should be higher in tropical lineages compared with extratropical lineages.

134 The Tropical Conservatism Hypothesis (TCH) (Pianka, 1966; Wiens & Donoghue,
135 2004) posits that the relative youth of colder temperate biomes combined with the inertia of
136 niche evolution (phylogenetic niche conservatism: Wiens & Graham, 2005; Losos, 2008) has
137 limited the accumulation of diversity in the temperate zone. In this scenario, net
138 diversification rates or equilibrium levels do not necessarily vary with latitude, and the
139 difference in richness is mainly due to time for diversification (Stephens & Wiens, 2003).
140 This idea is based on the fact that historically the Earth has been much warmer than it is now,
141 and much of what is now the temperate zone was covered by “megathermal” biomes. This
142 hypothesis is supported by the fossil record; many lineages that used to occur in the
143 Palearctic are now limited to tropical latitudes. This is true for ants as well; the Baltic amber
144 ant fauna from the late Eocene has greater affinity to modern Indo-Australian faunas than
145 modern Palearctic faunas (Guénard et al., 2015). The main prediction of this hypothesis is
146 that the ancestral region of most groups is the tropics (or areas with what we recognize now
147 as “tropical” climates that may have previously extended out of the tropics), transitions out of
148 the tropical zone are rare, and thus the temperate clades are younger and nested within
149 tropical clades. Transitions from tropical to temperate zones should be difficult because of
150 the many nontrivial adaptations that ectothermic organisms need to survive at higher
151 latitudes. An additional prediction of the TCH is that the accumulation of lineages in the
152 temperate zone through dispersal or cladogenesis has mostly occurred after the Oligocene
153 cooling, 34mya.

154 The Ecological Regulation Hypothesis (ERH) posits that, due to causal factors that
155 vary with latitude, more species can coexist locally and regionally in tropical ecosystems than
156 in temperate ecosystems. In this case, diversity is saturated at or near an ecological limit, and
157 this “carrying capacity” of species varies with latitude. Equilibrium diversity levels may be
158 regulated by factors such as productivity, perhaps mediated through competition and limiting
159 similarity (Pianka, 1966; Hurlbert & Stegen, 2014b; Rabosky & Hurlbert, 2015). Speciation
160 and extinction rates may vary over time to regulate richness at the requisite equilibrium level
161 for a geographic region, but a latitudinal factor acting on speciation/extinction is not causally
162 responsible for the disparity in diversity. Likewise, latitudinal affinity may be highly
163 conserved or evolve quickly, but it would be immaterial to the origins of the gradient if
164 diversity is saturated and regulated at levels that vary with latitude.

165 These hypotheses have been tested across broad taxonomic scales (e.g. birds: Jetz et
166 al., 2012, amphibians: Pyron & Wiens 2013; mammals: Buckley & Jetz, 2007; Rolland et al.,
167 2014), and predictions of the DRH and TCH have been recently examined on the scale of all
168 ants using a comprehensive geographic dataset (Economo et al. 2018; also see Moreau & Bell
169 2013; Pie 2016). That study found that tropical lineages are more ancient than extratropical
170 lineages, which mainly arose since the Oligocene cooling (past 34my), consistent with the
171 TCH. Further, they found that diversification rate was highly heterogeneous but uncorrelated
172 with latitude among ant clades, inconsistent with the DRH. Due to the limitations of
173 phylogenetic data at such broad taxonomic and time scales, they could not test for ecological
174 regulation (ERH). As with other studies on broad taxonomic scales, the analyses across all
175 ants provided the statistical advantages of big datasets and a deep-time perspective. However,
176 deep-time analyses also can be confounded by the fact that many ecological, functional trait,
177 and historical factors may affect macroevolutionary rates in ways that could obscure
178 underlying latitudinal effects. For example, ant diversification rates have been shown to be
179 heterogeneous across clades (Pie & Tschá, 2009; Moreau & Bell, 2013) and possibly related
180 to functional traits (Blanchard & Moreau, 2017). Analyses of closely related lineages allow
181 us to control to some extent for differences in biology unrelated to the variable of interest (in
182 this case latitudinal affinity), while the large trees of hyperdiverse radiations enhance
183 statistical power to detect trait-dependent diversification (Gamisch, 2016). Moreover,
184 latitudinal gradients are often present within individual clades that evolved recently
185 (Economo et al., 2015a), and different ecological and evolutionary dynamics can dominate at
186 different phylogenetic scales (Graham et al., 2018). Studies across broad phylogenetic/time
187 scales may miss the relevant scale of variation in diversification rate. Thus, the analysis of
188 closely related lineages within younger, hyper-rich radiations provides an important
189 complement to studies of larger taxa and longer time scales.

190 The global radiation of Pheidole arose entirely since the Oligocene cooling (last
191 34my), during which time it has evolved a latitudinal gradient echoing the pattern for all ants
192 (Economo et al., 2015a). Thus, Pheidole presents an opportunity to examine diversification
193 dynamics in this most recent period since the Oligocene, a period when many ant lineages
194 transitioned out of the tropics. While the low number of older extratropical ant lineages is
195 consistent with the TCH (Economo et al., 2018), there is still an open question of whether
196 niche conservatism, diversification rate differences, or ecological saturation explain the
197 emergence of the gradient since the Oligocene. According to the TCH, the tropical ancestry
198 of Pheidole combined with a low rate of evolution in latitudinal affinity (i.e. high

199 phylogenetic niche conservatism) explains why there are more species in the tropics in the
200 absence of latitudinal differences in macroevolutionary rates or regulation at different levels.
201 The DRH predicts that Pheidole is diversifying more rapidly in the tropics, and this explains
202 the current observed disparity in richness. The ERH posits that diversity is saturated at
203 different levels across latitudes, and thus we should see a period of high net diversification
204 rates early in the radiation followed by declines to near zero as richness reaches steady state
205 or “carrying capacity”. The ERH is thus an equilibrium hypothesis while the DRH and TCH
206 are both non-equilibrium hypotheses.

207 Here, we reconstruct a new global Pheidole phylogeny—the most comprehensive to
208 date—increasing substantially the taxonomic and geographic coverage from previous studies
209 of the genus (Moreau, 2008; Sarnat & Moreau, 2011; Economo et al., 2015a; Economo et al.,
210 2015b). We use the new phylogeny and geographic data from the GABI database to test
211 predictions of the three umbrella hypotheses for the latitudinal gradient. As mechanisms
212 involved with different hypotheses can be simultaneously operating (for example, speciation
213 rate can vary with latitude even while niche conservatism limits colonization of the
214 extratropics), our goal is to rule out mechanisms rather than isolate a single exclusive answer.
215 The analysis of this famously hyperdiverse radiation will advance our general understanding
216 of the latitudinal gradient, the most pervasive pattern of life on Earth.

217

218 **METHODS**

219

220 **Geographic Data**

221 Our geographic data are based primarily on the Global Ant Biodiversity Informatics Project
222 (GABI) database (Guénard et al., 2017) which can be viewed through the website
223 antmaps.org (Janicki et al., 2016), and secondarily on the personal collection records of the
224 authors (all of which are available on AntWeb.org). The former focuses on described species,
225 while the second was used to supplement data on morphospecies for taxa included in the
226 phylogenetic analysis. Because many records of ant occurrence are not associated with
227 geocoordinates, we assigned each record to a system of 415 polygons around the world
228 (Figure 1). Latitudinal range for a species was estimated as minimum and maximum
229 latitudes over all polygons in which a species occurs, excluding occurrences where the
230 species is considered exotic and dubious records. For statistical analyses, we used either the
231 absolute midpoint latitude of the range, an index of tropicality (fraction of latitudinal range in
232 the tropics – fraction of latitudinal range outside the tropics, with +/-23.5° latitude as the

233 boundary of the tropics). For tests using a binary coding latitudinal state, we used midpoint
234 latitude within or outside $\pm 23.5^\circ$ to separate tropical and extratropical taxa.

235

236 **Phylogeny reconstruction**

237 **Taxon Selection:** Compared with many other large ant radiations, the effort to reconstruct the
238 phylogenetic history of Pheidole is relatively far along. A series of studies, beginning with
239 Moreau (2008) and followed by others (Sarnat & Moreau, 2011; Economo et al., 2015a;
240 Economo et al., 2015b) has produced a broad picture of the evolutionary history of the genus.
241 However, for the purposes of understanding geographic patterns of diversification, having a
242 larger, and more proportionally sampled phylogeny will provide additional statistical power
243 and more robust results. Thus, we continued sampling Pheidole taxa for sequencing, focusing
244 on sampling more taxa from the Neotropics, Madagascar, and SE Asia, which had been
245 undersampled in previous analyses. In all, we increased the number of species from 282 taxa
246 in the most recent global Pheidole phylogeny (Economo et al., 2015a) to 449 taxa in the
247 current contribution (Table S2).

248

249 **Estimation of Sampling Completeness:** One source of uncertainty in large-scale analyses of
250 diversity is bias in taxonomic completeness overall and among different areas, particularly in
251 relatively poorly known groups such as insects. While there is still a pronounced latitudinal
252 gradient in Pheidole even among described species, there are undoubtedly many undescribed
253 species in the genus, and it is probable they are disproportionately found in the tropics. While
254 accounting for unobserved species is a challenge in any analysis, we devised an approximate
255 method to calculate sampling completeness across areas given the information available, and
256 use these estimates in our analysis of diversification rate. The details of our calculation are in
257 the Supporting Information.

258

259 **DNA Sequencing:** Previous molecular work (Moreau 2008, Sarnat & Moreau 2011,
260 Economo et al. 2015a) on Pheidole has generated a dataset based on eight nuclear loci
261 [His3.3B (histone H3.3B F1 copy), Lop1 (long wavelength sensitive opsin 1), GRIK2
262 (glutamate receptor ionotropic, kainate 2-like), unc_4 (unc-4 homeodomain gene), LOC15
263 (uncharacterized locus LOC15), CAD (carbomoylphosphate synthase), EF-1 α F2 (elongation
264 factor 1-alpha F2), Top1 (DNA topoisomerase 1)], and one mitochondrial locus [CO1
265 (cytochrome oxidase 1)]. In a previous study (Economo et al. 2015a), all 9 loci were

266 sequenced for a subset of 65 taxa representing the main Pheidole lineages around the world,
267 while three loci (COI, Lop1, and His3.3B) were sequenced for all taxa to fill out the clades
268 (217 taxa). This hierarchically redundant sampling design was chosen for reasons of cost and
269 time efficiency and to maximize the number of taxa, combined with the fact that many of the
270 slow-evolving nuclear genes provide less information on recent divergences.

271 We added 167 new Pheidole taxa to this existing dataset by extending this sampling
272 design and sequencing COI, Lop1, and His3.3B. We did not plan to sequence all 9 loci unless
273 we found novel divergent clades not represented by taxa with all 9 genes sequenced in the
274 earlier study (and we did not). Ant samples from field collections fixed in 95% EtOH were
275 extracted for DNAs using DNeasy Blood & Tissue Kit (Qiagen, Hilden, Germany). The
276 whole ant body was incubated in the extraction buffer without grinding during the first step,
277 and then the complete ant specimen was removed before filtering and cleaning the extracts
278 via a provided column. Extracted DNAs were subsequently used for PCR reactions for one
279 mitochondrial (CO1) (Folmer et al., 1994) and two nuclear (His3.3B and Lop1) regions. Each
280 reaction contained 0.5 ul of extracted DNA, 1ul of 10 × buffer, 0.75 ul of MgCl₂, 0.5 ul of
281 10mM dNTPs, 0.2 ul of 1% BSA, 0.4ul of each primer, 0.04ul of Tag DNA polymerase
282 (Invitrogen, USA), and ddH₂O to make a total of 10 ul reaction. Standard PCR procedures
283 were employed with annealing temperatures of 52, 60, and 60 C for CO1, His3.3B, and Lop1
284 regions, respectively. The amplicons were sequenced via a ABI³⁷⁰⁰ machine by the
285 Sequencing Core at the University of Michigan. Sequences were checked using SeqMan
286 (DNASTar Inc., USA).

287
288 Phylogenetic tree inference: We used Bayesian methods to infer a dated Pheidole phylogeny
289 including 449 ingroup taxa (Table S2). To generate codon-aware alignments for these loci,
290 we first searched NCBI's non-redundant CDS database (Clark et al., 2016) for reliable amino
291 acid sequences for all loci and retrieved such sequences for seven of the nine loci with the
292 following accession numbers: AIM2284.1 (CAD), ABW70333.1(CO1), EZA53539.1 (EF-1α
293 F2), EGI60526.1 (His3.3B), ABW36758.1 (Lop1), EGI59282.1 (unc-4), and AIM43286.1
294 (Top1). These sequences were used as references for generating codon-aware alignments.
295 The CAD, unc-4, and Top1 alignments generated using MAFFT v7.205 (Katoh & Standley,
296 2013) (--retree 4; --maxiterate 1000) showed no frameshift mutations and/or insertions and
297 deletions. However, the CO1, EF-1α F2, His3.3B, and Lop1 alignments did not match the
298 reference sequences, showing disruptions in the translated amino acid alignments (such as the
299 presence of numerous stop codons). For these loci, we used a codon-aware alignment

300 software, MACSE v1.01b (Ranwez et al., 2011), to generate the alignments. Reverse
301 translations of the reliable amino acid reference sequences, accounting for all possibilities at
302 each codon position, were passed as reliable input sequences to the software, we were able to
303 assign codon positions within the exons in these seven loci. The resulting alignments were
304 manually inspected and cleaned using Geneious R8 software. Furthermore, we identified,
305 extracted, and separately aligned intronic regions wherever necessary. The remaining two
306 loci, LOC15 and GRIK-2, were aligned using MAFFT. We concatenated all nine alignments
307 and once again manually cleaned the master alignment, resulting in an alignment containing
308 8839 sites.

309 We used PartitionFinder v1.1.1 (Lanfear et al., 2012) to determine the partitioning
310 scheme and corresponding models of molecular evolution. The model scope included HKY,
311 HKY+ Γ , SYM, SYM+ Γ , GTR, GTR+ Γ , TrN, TrN+ Γ , K80, K80+ Γ , TrNef, TrNef+ Γ , JC, and
312 JC+ Γ , branch lengths were set to 'linked', and model selection and comparison was set to
313 Bayesian Information Criterion (BIC). PartitionFinder identified an optimal scheme
314 containing 16 partitions (Table S3). We used ClockstaR (Duchêne et al., 2014) to determine
315 the optimal number of clock models across our partitions for relaxed-clock phylogenetics,
316 and a single linked clock was preferred based on the SEMmax criterion.

317 Our primary phylogenetic inference was conducted in BEAST2 v2.1.3 (Bouckaert et
318 al., 2014), but we first performed maximum likelihood (ML) reconstruction in RAXML
319 v8.0.25 (Stamatakis, 2014). Using the partitioning scheme described above and the GTR+ Γ
320 model, we ran 75 ML inferences with 1000 bootstraps to find the ML tree. Using the chronos
321 function in the ape package in R (Paradis et al., 2004), we scaled the tree by calibrating the
322 root node to a range of 50-60my. This tree was used as the starting tree for the BEAST2
323 analyses, but the topology was not fixed.

324 Unfortunately there are no reliable fossil calibrations available to date nodes within
325 the genus. Thus, the age of the group can only be informed by the age of the stem node and
326 information from fossils in related taxa across the subfamily Myrmicinae. Because our
327 analysis is concentrated within Pheidole, we preferred to use the stem node age distribution
328 (i.e. the most recent common ancestor of Pheidole and its sister lineage
329 Cephalotes+Procryptocerus) inferred as in a much larger analysis of the subfamily
330 Myrmicinae (Ward et al., 2015) that could make use of a broad range of molecular and fossil
331 data. Following those results, the stem node calibration was set to a normal distribution
332 (mean: 58.0 mya, sigma, 4.8my). Further analysis of the Pheidole fossil record with a goal to
333 place fossil taxa within the Pheidole phylogeny and refine dating of different nodes in the

334 tree, represents an important need for future phylogenetic work on the genus. Despite this
335 limitation, the analyses in this paper depend mostly on relative—rather than absolute—ages,
336 and we draw no conclusions based on the precise timing of nodes in the tree.

337 We used a relaxed lognormal clock model linked across partitions (due to the
338 ClockstaR results), and used the partitioning scheme and models identified with
339 PartitionFinder. Six independent analyses were run and chains were stopped between 45 and
340 80 million generations, after we observed convergence using Tracer software v1.6.0
341 (Rambaut 2014). We discarded the leading 33% of saved states as burnin, combined the
342 remaining trees from all runs to create the posterior set, and generated the Maximum Clade
343 Credibility tree and nodes set to median height. After pruning the outgroup, this tree was used
344 for all subsequent analyses.

345

346 **Macroevolutionary rate inference**

347 We took several complimentary approaches to estimating macroevolutionary rates
348 and potential dependencies on latitude, primarily basing our analysis on BAMM (Bayesian
349 Analysis of Macroevolutionary Mixtures, Rabosky, 2014), HiSSE (Hidden State Speciation
350 and Extinction, Beaulieu & O'Meara, 2016), and FiSSE (Rabosky & Goldberg, 2017), with a
351 secondary analysis using GeoSSE (Geographic State Speciation and Extinction, Goldberg et
352 al., 2011). These methods each have their strengths and weaknesses thus our approach is to
353 use them collectively to seek conclusions about our data that are robust to methodological
354 assumptions and implementation.

355 The main advantage of BAMM is that complex mixture models can be assessed with
356 rate shifts across the tree, including potentially accelerating and/or decelerating
357 diversification rates. While trait-dependent diversification models are not fit directly, trait-
358 diversification correlations can be assessed post hoc using structured rate permutations that
359 estimate correlations while accounting for phylogenetic dependency (Rabosky & Huang,
360 2015). We use BAMM to test for correlations between latitude and net diversification rate,
361 and evaluate evidence of decelerating diversification to a steady state (ecological regulation
362 of diversity) overall and in relation to the colonization of continents.

363 While BAMM has strengths in inferring complex mixtures of diversification
364 processes, they are not explicitly trait-dependent, and the SSE family of methods explicitly
365 fits models of trait-dependent diversification. SSE methods have been developed with
366 different kinds of trait data, either based on binary traits (BISSE, Maddison et al., 2007),
367 continuous traits (QuaSSE, FitzJohn, 2010), or explicitly geographic traits (GeoSSE,

368 Goldberg et al., 2011). While these methods are explicitly for inferring trait-dependent
369 speciation and extinction, they have the problem that differences in the focal trait are the only
370 mechanisms that can cause shifts in macroevolutionary rates. If the real process has complex
371 rate shifts then a more complex trait dependent model may fit better than a homogeneous null
372 model, even if the shifts are not related to the traits per se, leading to type-I errors (Rabosky
373 & Goldberg, 2015). These problems are at least partially solved by HiSSE (Beaulieu &
374 O'Meara, 2016), a method that fits binary trait-dependent speciation and extinction models
375 that can be formally tested against similarly complex trait-independent models. We thus
376 primarily used HiSSE for our analysis. Since GeoSSE has been implemented for explicitly
377 geographic dynamics, we also fit that model as a secondary test and present that analysis in
378 the supplement.

379 Finally, as an additional test for variation in speciation rate with latitude, we used a
380 non-parametric method, FiSSE (Rabosky & Goldberg, 2017), that does not depend on an
381 assumed model structure and is robust to false inferences of trait-dependent evolution given a
382 range of underlying complex evolutionary dynamics. FiSSE is limited to testing speciation
383 rate differences; it does not directly test for net diversification rate differences. However,
384 many (but not all) hypotheses for why diversification rate could vary with latitude are based
385 on mechanisms acting on speciation rate, so it is a partial test of the broader Diversification
386 Rate Hypothesis.

387

388

389 BMM implementation: We estimated net-diversification, speciation, and extinction rates
390 through time for the inferred Pheidole tree using the program BMM V2.5. The initial
391 values for speciation rate, rate shift, and extinction rate were estimated using the
392 setBMMpriors function from the R package BMMtools (Rabosky et al., 2014).
393 Specifically, a total of 2×10^8 generations of rjMCMC searches with samples stored every
394 8000 generations were performed using speciation-extinction. A total of 1000 post burnin
395 samples (50%) were retained. We performed two BMM runs for each of three assumptions
396 about sampling completeness (L, M, H) accounted for by changing the
397 GlobalSamplingFraction parameter (0.3, 0.22, 0.18, respectively, see Supplemental
398 Information for justification). To account for potential oversampling of Nearctic species, we
399 performed a series of runs where we lowered the number of Nearctic species by randomly
400 pruning 21 (of total 48) Nearctic tips from the tree ten times and performed a BMM run on
401 each replicate, using the M assumption for the GlobalSamplingFraction parameter.

402 Using the posteriors generated from these MCMC runs, we sought to 1) explore the
403 overall pattern of Pheidole diversification, 2) assess whether there is evidence of diversity
404 regulation, particularly decelerating diversification to zero over time and after colonization of
405 new areas, and 3) test for latitudinal dependency in diversification rate while accounting for
406 phylogenetic non-independence. We visualized the lineage specific diversification with the
407 `plot.bammdata` function from BMMtools, and the time plot of clade-specific diversification
408 rate was plotted with the `plotRateThroughTime` function. We used STRAPP (e.g. the
409 `traitDependentBMM` function in BMMtools) to test for significance of any latitude-
410 diversification correlations. We tested for diversification rate vs. either tropicality index or
411 absolute midpoint latitude (one-tailed, 10000 iterations, Spearman's rho as test statistic). We
412 also checked whether our results were robust to using Pearson correlation as test statistic or
413 coding latitude as a binary variable (`tropicality>0` or `tropicality<0`) and using Mann-Whitney
414 test.

415

416 HiSSE Implementation: The HiSSE approach (Beaulieu & O'Meara, 2016) extends the
417 BiSSE (Binary State Speciation and Extinction model) (Maddison et al., 2007) framework
418 with two advances. First, the HiSSE model itself allows for more complex models in which
419 macroevolutionary rates can be the function of the focal trait and a hidden state. Thus, if our
420 focal character has states 1 and 0 (in our case tropical and extratropical), there could be an
421 influence of a second unobserved character (with states A and B) on a macroevolutionary
422 rates λ and μ (λ_{0A} , λ_{0B} , λ_{1A} , λ_{1B}). Second, importantly, it allows the fitting of null character-
423 independent models (CID) in which a hidden factor(s) underlies diversification rate changes
424 without the influence of the focal trait under investigation. This allows trait-dependent BiSSE
425 models to be compared to a character-independent model of similar complexity (CID-2, with
426 two hidden states A and B) and more complicated HiSSE models to be compared to models
427 of similar complexity (CID-4, with four hidden states A, B, C, D). BiSSE (trait dependent
428 speciation-extinction), HiSSE (trait-dependent speciation/extinction with hidden states that
429 also affect speciation/extinction) and CID (trait-independent models with hidden states that
430 affect speciation/extinction) are best used together and models with all structures can be
431 compared.

432 We fit a range of models with increasing complexity, starting with the BiSSE family
433 of models under the following sets of constraints on the parameters: all diversification and
434 transition rates equal among states, diversification equal but transition rates different (i.e.

435 speciation and or extinction changes with latitude, but transition rates among temperate and
436 tropical are equal), diversification different but transition rates equal (i.e. speciation and
437 extinction vary with state, but transition rates are equal), or all rates free unconstrained to
438 vary with state (the full BiSSE model).

439 The HiSSE models allow speciation/extinction/transition rates to vary with the focal
440 trait and also among two hidden traits. One question in implementing HiSSE is how to set the
441 transition parameters among states (combination of observed 0/1 and hidden A/B states, with
442 combined state space 0A, 1A, 0B, 1B). We followed suggestions of the authors of the method
443 (Beaulieu & O'Meara, 2016), either setting all transition rates to be equal, or assumed a three
444 parameter rates in which transitions between the observed states could vary but transitions
445 between hidden states is a single parameter. The CID-2 and CID-4 models are fit including 2
446 or 4 hidden states, respectively, but with no dependence on the observed traits. For these, we
447 also assumed alternatively a single rate for all state transitions (observed and hidden) or a
448 three-rate model including two rates for transitions between the observed states and one
449 between all hidden states.

450 We implemented all of the above analyses using functions in the R package hisse
451 (Beaulieu & O'Meara, 2016). As with the BAMM analysis, we ran all models using either the
452 (L, M, H) assumptions about sampling completeness, and analyzed both the global Pheidole
453 and New World only. For the New World analyses, we additionally adjusted the sampling
454 fraction (M^*) to account for possible undersampling of tropical species relative to
455 extratropical species. As the ML optimization does not always find the global minimum from
456 a single starting point, we ran 20 ML searches for each model using random starting
457 parameters chosen from a uniform distribution on the interval (0,1). For all the models above,
458 we ran them alternatively assuming a fixed root in the tropical state, or root probability
459 estimated with the default “madwitz” method based on the data. As we found the results were
460 insensitive to the root method, we only present results with the default option. After all
461 BiSSE, HiSSE, and CID models were inferred, we compared all models with sample-size
462 corrected Akaike's Information Criterion (AICc) scores.

463
464 FiSSE Approach: FiSSE (Rabosky & Goldberg, 2017) is a nonparametric test for trait-
465 dependent speciation rates that does not assume an underlying model structure, but rather
466 depends on distributions of branch lengths in the different states. FiSSE is complementary to
467 the BiSSE and is robust to Type-I error. We performed both one-tailed and two-tailed tests of
468 FiSSE to test for speciation differences between extratropical and tropical taxa, using the

469 global Pheidole and only the New World Pheidole. We also performed FiSSE on a set of
470 trees for the New World only where temperate species were thinned to account for possible
471 undersampling of the tropics (see Supporting Information).

472

473 **Phylogenetic niche conservatism:** While previous studies have shown that Pheidole likely has
474 a tropical ancestor (Moreau 2008, Economo et al. 2015a), it remains an open question
475 whether phylogenetic niche conservatism is strong enough to produce a gradient pattern
476 during the Oligocene period, a key prediction of the TCH. We performed analyses to
477 evaluate the degree to which latitudinal affinity is phylogenetically conserved in Pheidole,
478 and used simulations to test if that conservation is strong enough for a gradient to emerge
479 given tropical ancestry alone. For this, we first calculated two measures of phylogenetic
480 signal—Blomberg’s K (Blomberg et al., 2003) and Pagel’s lambda (Pagel, 1999)—treating
481 absolute latitudinal midpoint as a continuous trait, using the `phylosig()` function in the R
482 package `phytools` (Revell, 2012). Second, to estimate the overall evolutionary rates, we fit
483 models of discrete character evolution (treating latitudinal affinity as a binary variable) using
484 the `fitDiscrete()` function in the R package `geiger` (Pennell et al., 2014). To visualize the
485 evolution of latitudinal affinity, we performed 100 stochastic character maps on the empirical
486 tree using the `make.simmap()` function, and plotted a summary of state probabilities with the
487 function `densityMap()`, both from the `phytools` package. Finally, to estimate whether the
488 inferred rate of evolution combined with tropical ancestral state is consistent with the
489 observed richness difference even in the absence of diversity regulation and diversification
490 rate differences, we simulated niche evolution on the empirical tree and maximum likelihood
491 model with the `sim.history()` function from `phytools`. While tree shape and trait state are not
492 necessarily independent (i.e. the dependent model is implemented in the BiSSE/HiSSE
493 analyses), this analysis asks whether we would be likely to observe a gradient even if they
494 were independent, given that Pheidole likely has a tropical ancestor and given the rate that
495 latitudinal affinity evolves. Pheidole likely has a tropical ancestor as *Pheidole fimbriata*,
496 which is sister to the rest of Pheidole, and the sister lineage of Pheidole, *Cephalotes* +
497 *Procryptocerus*, are all tropical (Moreau, 2008; Ward et al., 2015).

498

499 **RESULTS**

500 Pheidole exhibits a latitudinal diversity gradient that is overall similar to ants as a
501 whole (Fig. 1). The BEAST analysis inferred a phylogeny whose major features are
502 consistent with previous studies (Figs. 2, S1). The crown age of the group (i.e. the mrca of

503 *Pheidole fimbriata* with the rest of *Pheidole*) is inferred here to be younger than in a previous
504 study (~29mya vs. ~37mya in Economo et al., 2015a).

505 According to the BAMM analysis, the hyperdiversification of *Pheidole* began after an
506 acceleration approximately 15-16 mya, and all species except for two early-diverging
507 lineages (*P. fimbriata* and *P. rhea*) are descended from this event (Figure 2). Diversification
508 initially occurred in the New World, exhibiting a decelerating trend over time. Around
509 13mya, a single lineage colonized the Old World and this was associated with another burst
510 of diversification followed by a slowdown in a clade encompassing Asia and Africa.
511 Madagascar and Australia-NG were later colonized, followed by accelerations and
512 subsequent decelerations in each clade (Figs. 2, S1, S2). There were several other
513 accelerations that were not obviously associated with geographic transitions, including one
514 clade in the New World and the megacephala group in the Afrotropics. This general pattern
515 of sequential colonization-acceleration-deceleration pattern is robust to changing the
516 sampling fraction parameter, although as one would expect, the inferred degree of
517 deceleration becomes less pronounced if one assumes that more species are left to be
518 sampled. However, there is no evidence that diversity is saturated (i.e. net diversification rate
519 approaching zero) as net diversification rates were all strongly positive (ranging between 0.2-
520 0.5 across regions and analyses with different parameter assumptions).

521 The extratropical lineages generally belong to young clades nested within larger
522 tropical clades (Figs. 2, S1). While diversification rates vary across the genus to a degree, we
523 could not detect a significant correlation (assessed with STRAPP) between BAMM-inferred
524 net diversification rate and either absolute midpoint latitude or tropicality index across any of
525 the analyses we performed (Fig. 3). These results were similar across variation in the
526 assumed global sampling fractions, whether we calculated correlations for individual clades
527 or the whole tree, and including trees where Nearctic species were culled to account for
528 possible uneven sampling. Although significance tests were one-tailed for higher
529 diversification in the tropics, we also note that none of the observed correlation coefficients
530 were outside the null range in either direction.

531 The HiSSE analysis was also broadly consistent with BAMM analysis in finding no
532 statistical support for a correlation between macroevolutionary rates and latitude. In general,
533 the CID-2 trait-independent null model outperformed the BiSSE trait-dependent models, and
534 the CID-4 null outperformed the HiSSE trait-dependent models, and the CID-4 models had
535 the global minimum AICc across the different permutations of the analysis (Table 1). Thus,
536 this analysis provided no evidence for latitude-dependent macroevolution in this genus. It is

537 worth noting as well that the AIC-minimizing versions of the BiSSE and HiSSE models,
538 which again were themselves not preferred over the null models, generally did not support
539 higher diversification rate in the tropics. The BiSSE model detected a slightly higher
540 diversification rate in the extratropical zone and the HiSSE model either fit models where
541 tropical diversification was higher than extratropical while in one hidden state and lower in
542 the other hidden state, or where the extratropical diversification was always higher in both
543 hidden states. For the New World, use of the sampling effort correction removed this slight,
544 and non-significant difference. The GeoSSE analysis showed overall similar results to
545 BiSSE, with a positive latitude-diversification rate trend in the New World, but not global,
546 Pheidole; however, the association is not robust to the correction for latitudinal
547 undersampling (see supplement).

548 The FiSSE analysis was also consistent with the other analyses in showing no
549 correlation between speciation rate and latitude for global Pheidole ($\lambda_{\text{temp}}=0.28$, $\lambda_{\text{trop}}=0.27$,
550 two tailed $p>0.88$), but did show a positive speciation-latitude correlation for the New World
551 alone ($\lambda_{\text{temp}}=0.30$, $\lambda_{\text{trop}}=0.20$, two-tailed $p<0.026$). However, when we dropped extratropical
552 tips from the phylogeny to simulate potential latitudinal undersampling of the tropics, this
553 difference was much more modest and no longer significant ($n=10$, mean $\lambda_{\text{temp}}=0.24$,
554 S.E.=0.005, mean $\lambda_{\text{trop}}=0.20$, S.E. = 0.0002, p range: 0.19-0.72 among replicates).

555 The extratropical lineages are clustered with each other on the tree, although it is clear
556 there were numerous transitions out of the tropics (Fig. 4). The tests for phylogenetic signal
557 in latitudinal affinity for Blomberg's K ($K=0.34$, $p<0.002$) and Pagel's lambda ($\lambda=0.95$,
558 $p<10^{-57}$) were both highly significant. Symmetric and asymmetric models of discrete
559 character evolution both fit the data comparably well (symmetric model $q_{\text{trop}\rightarrow\text{etrop}}=q_{\text{etrop}\rightarrow\text{trop}}$
560 $=0.015$, AICc=235.5, asymmetric model $q_{\text{trop}\rightarrow\text{etrop}}=0.013$, $q_{\text{etrop}\rightarrow\text{trop}}=0.060$,
561 AICc=234.9). Simulations of character evolution on the empirical phylogeny show that a
562 latitudinal gradient is the most common outcome if one assumes a tropical ancestor and either
563 model for the inferred rate of evolution of latitudinal affinity (Fig. 4).

564

565 DISCUSSION

566 Our analysis of Pheidole macroevolution sheds light on the mechanisms responsible
567 for the evolution of the latitudinal diversity gradient in ants. By focusing on the dynamics of
568 a massive radiation in the post-Oligocene, our study complements taxon-wide studies that
569 focus on differences among highly divergent clades and deeper timescales (e.g. Cardillo et

570 al., 2005; Weir & Schluter, 2007; Jetz et al., 2012; Pyron & Wiens, 2013; Rolland et al.,
571 2014; Kerkhoff et al. 2014, Duchêne & Cardillo, 2015; Economo et al., 2018).

572 We find no evidence of higher diversification rate for tropical Pheidole lineages
573 across any of our analyses (Figs. 2-4, S1), as would be predicted by the Diversification Rate
574 Hypothesis. In general, the signal of latitude as a trait affecting macroevolutionary rates in
575 the BAMM, HiSSE, and FiSSE analyses was weak to non-existent. When there was some
576 hint of a correlation, for example in the best fitting (but still not better than null)
577 HiSSE/BiSSE analyses, and the FiSSE analysis for New World speciation rate uncorrected
578 for latitudinal sampling bias, it was in the direction of higher diversification/speciation in the
579 temperate zone. However, those correlations were not robust to reasonable assumptions about
580 undersampling in the tropics, thus the overall picture is a lack of evidence for latitudinal
581 dependency for macroevolutionary rates.

582 We do not view our analysis as ruling out that such systematic macroevolution-
583 latitude relationships may exist, even in Pheidole. Rather, our analysis only suggests that
584 such relationships are not the causal factor in the gradient. The Diversification Rate
585 Hypothesis assumes that lineages reach different latitudes early on in their evolution, and the
586 disparity of richness is due to different accumulation rates over time. If niche conservatism is
587 too high for lineages to evolve out of the tropics (or vice versa) early on in the radiation, there
588 may be no chance for any latitude-macroevolutionary rate correlations to manifest and be
589 statistically detectible. Thus, we view our analysis as stronger evidence that a diversification
590 rate-latitude correlation is not causal in the latitudinal gradient in Pheidole, rather than
591 showing that no such relationship exists. The finding that a latitudinal gradient in
592 diversification rates does not underlie the diversity gradient in Pheidole echoes similar results
593 for birds (Weir & Schluter, 2007; Jetz et al., 2012; Rabosky & Huang, 2012), butterflies
594 (Owens et al., 2017), marine fishes (Rabosky et al., 2018; but see Siquera et al., 2016).
595 However, other recent work on mammals (Rolland et al., 2014), amphibians (Pyron & Wiens,
596 2013), and studies on the fossil record (e.g. Jablonski et al., 2006) that indicated elevated net
597 diversification rates in the tropics. Thus, there continues to be disagreement across studies
598 and taxonomic groups. Whether this reflects true process variation across clades or
599 differences in conceptual and methodological approaches across studies remains an open
600 question.

601 Contemporary net diversification rates are positive in Pheidole across all regions,
602 with current rates varying between 0.25-0.50 across regions and assumptions about missing
603 taxa. This contradicts a key proposition of the Ecological Regulation Hypothesis, that

604 diversity is at an equilibrium “carrying capacity” across regions (Pianka, 1966; Hurlbert &
605 Stegen, 2014b; Rabosky & Hurlbert, 2015). There is evidence, however, that ecological
606 opportunity at least partially controls diversification rate in Pheidole. Specifically, each time
607 a new continent is colonized, diversification initially increases followed by a slowdown as
608 richness increases, which can be a sign of niche filling (but not necessarily, see discussions in
609 Moen & Morlon, 2014; Harmon & Harrison 2015). This could indicate that diversity will
610 eventually saturate at a steady state if net diversification rate continues to decrease (at current
611 rates of rate decrease, this would occur in about 10-20 million years). However, diversity
612 dependence is not in itself evidence of ecological limits (Harmon & Harrison, 2015), and it is
613 equally plausible that richness would not saturate but instead reach a peak and then decline,
614 resulting in a pulse or boom-bust pattern for the clade (e.g. as envisaged by Ricklefs, 2014).
615 The further investigation of the role of ecological limitations on diversity, and any latitudinal
616 differences in those limits, remains an important direction for future work. One promising
617 direction from a completely different angle would be to examine how niche overlap and
618 coexistence in Pheidole varies with latitude or energetic constraints, as has been pursued in
619 better studied taxa such as birds (e.g. Pigot et al., 2016), but the ant data are not yet available
620 at high enough resolution to pursue such analyses.

621 Overall, the results match the predictions of the tropical conservatism hypothesis
622 (TCH). We found that latitudinal affinity is moderately conserved in Pheidole. While there
623 have been a number of transitions from the tropics to the temperate zone, latitudinal affinity
624 evolves slowly enough to make a richness gradient the most likely outcome simply due to
625 tropical ancestry and phylogenetic inertia. Thus, our study joins a series of recent studies
626 supporting the TCH for woody plants (Kerckhoff et al., 2014), birds (Duchêne & Cardillo,
627 2015), mammals (Buckley et al., 2010), and butterflies (Hawkins & DeVries, 2009).

628 These results for Pheidole evolution in the post-Oligocene connect well to results on
629 ant diversification on deeper timescales (Economo et al., 2018), and together tell a coherent
630 story about the evolution of latitudinal gradients in ants across scales. Most ant lineages older
631 than 34mya are reconstructed to be tropical, including the Pheidole stem lineage. Around 15
632 mya, Pheidole exhibited a many-fold acceleration in diversification rate and began a massive
633 radiation. The reason for this initial acceleration, such as evolution of a key innovation,
634 remains unknown. It took time for some Pheidole lineages to evolve the requisite traits for
635 colonization of high latitudes. Once colonization of cold biomes occurred, diversification was
636 not detectibly slower. In their analysis across all ant clades, Economo et al. (2018) also found
637 no evidence for elevated net diversification rates among clades centered in the tropics relative

638 to those in the temperate zone, although clades are quite heterogeneous in rate, probably due
639 to other latent biological and historical differences. It remained possible that diversification
640 rate was correlated with latitude within the large clades, but biological differences among
641 clades obscured this pattern. Within Pheidole, diversification rate is much less
642 heterogeneous, but there is still no evidence of a negative latitudinal correlation, implying
643 that lack of phylogenetic resolution within large clades was not hiding this relationship in the
644 previous analysis (Economo et al. 2018). Further work is needed to unravel diversification
645 patterns of other hyperdiverse ant clades (e.g. Camponotus, Strumigenys, Tetramorium,
646 Crematogaster) that also exhibit strong latitudinal gradients to confirm this apparent
647 consistency across phylogenetic scales. Indeed, these five hyperdiverse genera (out of 334
648 total ant genera) constitute over a third of all ant described ant species (~5000), so each has a
649 marked effect on ant-wide patterns such as latitudinal gradients.

650 While our results are most consistent with tropical niche conservatism (TCH)
651 explaining the Pheidole latitudinal gradient, other patterns such as the diversification pulses
652 after colonization of new regions cannot be explained by phylogenetic niche conservatism
653 alone. Rather, even as our study rejects the main assertion of the ERH that contemporary
654 richness is regulated in steady state—Pheidole richness is apparently far from equilibrium
655 everywhere—we find evidence for an underlying mechanism of the ERH that diversity and
656 diversification are regulated by ecological opportunity and the filling of niche space. This
657 underscores the point that the mechanisms underlying the broad umbrella hypotheses are not
658 mutually exclusive, and even though a particular mechanism may not be causal for the
659 gradient, it may still be an important process operating in the diversification of different
660 groups, or operate on different phylogenetic scales in the same group (Graham et al., 2018).
661 Further quantitative approaches may be necessary to disentangle different mechanisms
662 operating simultaneously. We agree with the approach advocated by some (Hurlbert &
663 Stegen, 2014a) toward a quantitative formulation of multiple competing and intersecting
664 hypotheses, combined with a simulation-based approach to identify their key predictions. We
665 felt initial efforts in this direction were not yet mature enough to use as a basis for the current
666 study, but look forward to further development of the approach in the future.

667 Despite the high level of research effort directed toward understanding the latitudinal
668 gradient, the matter is far from resolved (Mittelbach et al., 2007). Studies have differed in
669 their conclusions about the origins of the gradient, probably due to both differences in
670 conceptual and methodological approaches and real variation in process and history across
671 taxonomic groups. The former should continue to improve as we develop more penetrating

672 quantitative methods that make use of more diverse data types. Variability across taxonomic
673 groups is best assessed and understood by examining more of them. With development of
674 global invertebrate datasets like the one analyzed here, we stand to broaden our perspective
675 on large-scale biological patterns and their origins.

676

677

678 **REFERENCES:**

679

680 Beaulieu, J.M. & O'Meara, B.C. (2016) Detecting hidden diversification shifts in models of
681 trait-dependent speciation and extinction. *Systematic Biology*, **65**, 583-601.

682 Blanchard, B.D. & Moreau, C.S. (2017) Defensive traits exhibit an evolutionary trade-off and
683 drive diversification in ants. *Evolution*, **71**, 315-328.

684 Blomberg, S.P., Garland, T. & Ives, A.R. (2003) Testing for phylogenetic signal in
685 comparative data: behavioral traits are more labile. *Evolution*, **57**, 717-745.

686 Bouckaert, R., Heled, J., Kuhnert, D., Vaughan, T., Wu, C.H., Xie, D., Suchard, M.A.,
687 Rambaut, A. & Drummond, A.J. (2014) BEAST 2: a software platform for Bayesian
688 evolutionary analysis. *PLoS Computational Biology*, **10**, e1003537.

689 Brady, S.G., Schultz, T.R., Fisher, B.L. & Ward, P.S. (2006) Evaluating alternative
690 hypotheses for the early evolution and diversification of ants. *Proceedings of the*
691 *National Academy of Sciences*, **103**, 18172-18177.

692 Buckley, L.B. & Jetz, W. (2007) Environmental and historical constraints on global patterns
693 of amphibian richness. *Proceedings of the Royal Society of London B: Biological*
694 *Sciences*, **274**, 1167-1173.

695 Buckley, L.B., Davies, T.J., Ackerly, D.D., Kraft, N.J.B., Harrison, S.P., Anacker, B.L.,
696 Cornell, H.V., Damschen, E.I., Grytnes, J.A., Hawkins, B.A., McCain, C.M.,
697 Stephens, P.R. & Wiens, J.J. (2010) Phylogeny, niche conservatism and the latitudinal
698 diversity gradient in mammals. *Proceedings of the Royal Society B: Biological*
699 *Sciences*, **277**, 2131-2138.

700 Cardillo, M., Orme, C.D.L. & Owens, I.P. (2005) Testing for latitudinal bias in diversification
701 rates: an example using New World birds. *Ecology*, **86**, 2278-2287.

702 Clark, K., Karsch-Mizrachi, I., Lipman, D.J., Ostell, J. & Sayers, E.W. (2016) GenBank.
703 *Nucleic Acids Research*, **44**, D67-D72.

704 Condamine, F.L., Sperling, F.A.H., Wahlberg, N., Rasplus, J.Y. & Kergoat, G.J. (2012) What
705 causes latitudinal gradients in species diversity? *Evolutionary processes and*

- 706 ecological constraints on swallowtail biodiversity. *Ecology Letters*, **15**, 267-277.
- 707 Duchêne, D.A. & Cardillo, M. (2015) Phylogenetic patterns in the geographic distributions of
708 birds support the tropical conservatism hypothesis. *Global Ecology and*
709 *Biogeography*, **24**, 1261-1268.
- 710 Duchêne, S., Molak, M. & Ho, S.Y.W. (2014) ClockstaR: choosing the number of relaxed-
711 clock models in molecular phylogenetic analysis. *Bioinformatics*, **30**, 1017-1019.
- 712 Dunn, R.R., Agosti, D., Andersen, A.N., Arnan, X., Bruhl, C.A., Cerdá, X., Ellison, A.M.,
713 Fisher, B.L., Fitzpatrick, M.C. & Gibb, H. (2009) Climatic drivers of hemispheric
714 asymmetry in global patterns of ant species richness. *Ecology Letters*, **12**, 324-333.
- 715 Economo, E.P., Klimov, P., Sarnat, E.M., Guenard, B., Weiser, M.D., Lecroq, B. & Knowles,
716 L.L. (2015a) Global phylogenetic structure of the hyperdiverse ant genus *Pheidole*
717 reveals the repeated evolution of macroecological patterns. *Proceedings of the Royal*
718 *Society B: Biological Sciences*, **282**, 20141416.
- 719 Economo, E.P., Sarnat, E.M., Janda, M., Clouse, R., Klimov, P.B., Fischer, G., Blanchard,
720 B.D., Ramirez, L.N., Andersen, A.N., Berman, M., Guenard, B., Lucky, A., Rabeling,
721 C., Wilson, E.O. & Knowles, L.L. (2015b) Breaking out of biogeographical modules:
722 range expansion and taxon cycles in the hyperdiverse ant genus *Pheidole*. *Journal of*
723 *Biogeography*, **42**, 2289-2301.
- 724 Economo, E.P., Narula, N., Friedman, N. R., Weiser, M. D., Guénard, B. (2018)
725 Macroecology and macroevolution of the latitudinal diversity gradient in ants. *Nature*
726 *Communications*, **9**, 1778.
- 727 Fine, P.V.A. (2015) Ecological and evolutionary drivers of geographic variation in species
728 diversity. *Annual Review of Ecology, Evolution, and Systematics*, **46**, 369-392.
- 729 FitzJohn, R.G. (2010) Quantitative traits and diversification. *Systematic Biology*, **59**, 619-
730 633.
- 731 Folmer, O., Black, M., Hoeh, W., Lutz, R. & Vrijenhoek, R. (1994) DNA primers for
732 amplification of mitochondrial cytochrome c oxidase subunit I from diverse metazoan
733 invertebrates. *Molecular Marine Biology and Biotechnology*, **3**, 294-299.
- 734 Gamisch, A. (2016) Notes on the statistical power of the Binary State Speciation and
735 Extinction (BiSSE) Model. *Evolutionary Bioinformatics Online*, **12**, 165-174.
- 736 Goldberg, E.E., Lancaster, L.T. & Ree, R.H. (2011) Phylogenetic inference of reciprocal
737 effects between geographic range evolution and diversification. *Systematic Biology*,
738 **60**, 451-465.
- 739 Graham, C.H., Storch, D., Machac, A. (2018) Phylogenetic scale in ecology and evolution.

- 740 Global Ecology and Biogeography, **27**, 175-187.
- 741 Guénard, B., Perrichot, V. & Economo, E.P. (2015) Integration of global fossil and modern
742 biodiversity data reveals dynamism and stasis in ant macroecological patterns.
743 Journal of Biogeography, **42**, 2302-2312.
- 744 Guénard, B., Weiser, M.D., Gomez, K., Narula, N. & Economo, E.P. (2017) The Global Ant
745 Biodiversity Informatics (GABI) database: synthesizing data on the geographic
746 distribution of ant species (Hymenoptera: Formicidae). Myrmecological News, **24**, 83-
747 89.
- 748 Harmon, L., & Harrison, S. (2015) Species diversity is dynamic and unbounded at local and
749 continental scales. American Naturalist, **185**, 584-593.
- 750 Hawkins, B.A. & DeVries, P.J. (2009) Tropical niche conservatism and the species richness
751 gradient of North American butterflies. Journal of Biogeography, **36**, 1698-1711.
- 752 Hurlbert, A.H. & Stegen, J.C. (2014a) On the processes generating latitudinal richness
753 gradients: identifying diagnostic patterns and predictions. Frontiers in Genetics, **5**
- 754 Hurlbert, A.H. & Stegen, J.C. (2014b) When should species richness be energy limited, and
755 how would we know? Ecology Letters, **17**, 401-413.
- 756 Jablonski, D., Roy, K., Valentine, J.W. (2006) Out of the tropics: evolutionary dynamics of
757 the latitudinal diversity gradient. Science, **314**, 102-106.
- 758 Janicki, J., Narula, N., Ziegler, M., Guenard, B. & Economo, E.P. (2016) Visualizing and
759 interacting with large-volume biodiversity data using client-server web-mapping
760 applications: The design and implementation of antmaps.org. Ecological Informatics,
761 **32**, 185-193.
- 762 Jetz, W., Thomas, G.H., Joy, J.B., Hartmann, K. & Mooers, A.O. (2012) The global diversity
763 of birds in space and time. Nature, **491**, 444-448.
- 764 Kaspari, M., Ward, P.S. & Yuan, M. (2004) Energy gradients and the geographic distribution
765 of local ant diversity. Oecologia, **140**, 407-413.
- 766 Katoh, K. & Standley, D.M. (2013) MAFFT Multiple sequence alignment software version 7:
767 Improvements in performance and usability. Molecular Biology and Evolution, **30**,
768 772-780.
- 769 Kerkhoff, A.J., Moriarty, P.E. & Weiser, M.D. (2014) The latitudinal species richness gradient
770 in New World woody angiosperms is consistent with the tropical conservatism
771 hypothesis. Proceedings of the National Academy of Sciences of the United States of
772 America, **111**, 8125-8130.
- 773 Lanfear, R., Calcott, B., Ho, S.Y.W. & Guindon, S. (2012) PartitionFinder: Combined

- 774 selection of partitioning schemes and substitution models for phylogenetic analyses.
775 *Molecular Biology and Evolution*, **29**, 1695-1701.
- 776 Losos, J.B. (2008) Phylogenetic niche conservatism, phylogenetic signal and the relationship
777 between phylogenetic relatedness and ecological similarity among species. *Ecology*
778 *Letters*, **11**, 995-1003.
- 779 Maddison, W.P., Midford, P.E. & Otto, S.P. (2007) Estimating a binary character's effect on
780 speciation and extinction. *Systematic Biology*, **56**, 701-710.
- 781 McKenna, D.D. & Farrell, B.D. (2006) Tropical forests are both evolutionary cradles and
782 museums of leaf beetle diversity. *Proceedings of the National Academy of Sciences*,
783 **103**, 10947-10951.
- 784 Mittelbach, G.G., Schemske, D.W., Cornell, H.V., Allen, A.P., Brown, J.M., Bush, M.B.,
785 Harrison, S.P., Hurlbert, A.H., Knowlton, N. & Lessios, H.A. (2007) Evolution and
786 the latitudinal diversity gradient: speciation, extinction and biogeography. *Ecology*
787 *Letters*, **10**, 315-331.
- 788 Moen, D., Morlon, H. (2014) Why does diversification slow down? *Trends in Ecology &*
789 *Evolution*, **29**, 190-197.
- 790 Moreau, C.S. (2008) Unraveling the evolutionary history of the hyperdiverse ant genus
791 *Pheidole* (Hymenoptera : Formicidae). *Molecular Phylogenetics and Evolution*, **48**,
792 224-239.
- 793 Moreau, C.S. & Bell, C.D. (2013) Testing the museum versus cradle tropical biological
794 diversity hypothesis: phylogeny, diversification, and ancestral biogeographic range
795 evolution of the ants. *Evolution*, **67**, 2240-2257.
- 796 Moreau, C.S., Bell, C.D., Vila, R., Archibald, S.B. & Pierce, N.E. (2006) Phylogeny of the
797 ants: diversification in the age of angiosperms. *Science*, **312**, 101-104.
- 798 Owens, H.L., Lewis, D.S., Dupuis, J.R., Clamens, A.L., Sperling, F.A.H., Kawahara, A.Y.,
799 Guralnick, R.P. & Condamine, F.L. (2017) The latitudinal diversity gradient in New
800 World swallowtail butterflies is caused by contrasting patterns of out-of-and into-the-
801 tropics dispersal. *Global Ecology and Biogeography*, **26**, 1447-1458.
- 802 Pagel, M. (1999) Inferring the historical patterns of biological evolution. *Nature*, **401**, 877-
803 884.
- 804 Paradis, E., Claude, J. & Strimmer, K. (2004) APE: Analyses of phylogenetics and evolution
805 in R language. *Bioinformatics*, **20**, 289-290.
- 806 Pennell, M.W., Eastman, J.M., Slater, G.J., Brown, J.W., Uyeda, J.C., FitzJohn, R.G., Alfaro,
807 M.E. & Harmon, L.J. (2014) geiger v2.0: an expanded suite of methods for fitting

808 macroevolutionary models to phylogenetic trees. *Bioinformatics*, **30**, 2216-2218.

809 Pianka, E.R. (1966) Latitudinal gradients in species diversity - a review of concepts.

810 *American Naturalist*, **100**, 33-&.

811 Pie, M.R. (2016) The macroevolution of climatic niches and its role in ant diversification.

812 *Ecological Entomology*, **41**, 301-307.

813 Pie, M.R., & Tschá, M.K. (2009) The macroevolutionary dynamics of ant diversification.

814 *Evolution*, **63**, 3023-3030.

815 Pigot, A.L., Tobias, J.A. & Jetz, W. (2016) Energetic constraints on species coexistence in

816 birds. *PLoS Biology*, **14**, e1002407.

817 Pyron, R.A. & Wiens, J.J. (2013) Large-scale phylogenetic analyses reveal the causes of high

818 tropical amphibian diversity. *Proceedings of the Royal Society of London B:*

819 *Biological Sciences*, **280**, 20131622.

820 Rabosky, D.L. (2014) Automatic detection of key innovations, rate shifts, and diversity-

821 dependence on phylogenetic trees. *PLoS ONE*, **9**, e89543.

822 Rabosky, D.L. & Hurlbert, A.H. (2015) Species richness at continental scales is dominated by

823 ecological limits. *American Naturalist*, **185**, 572-583.

824 Rabosky, D.L. & Goldberg, E.E. (2015) Model inadequacy and mistaken inferences of trait-

825 dependent speciation. *Systematic Biology*, **64**, 340-355.

826 Rabosky, D.L. & Huang, H. (2015) Minimal effects of latitude on present-day speciation

827 rates in New World birds. *Proceedings of the Royal Society of London B: Biological*

828 *Sciences*, **282**, 20142889.

829 Rabosky, D.L. & Goldberg, E.E. (2017) FiSSE: A simple nonparametric test for the effects of

830 a binary character on lineage diversification rates. *Evolution*, **71**, 1432-1442.

831 Rabosky, D.L., Grudler, M., Anderson, C., Shi, J.J., Brown, J.W., Huang, H. & Larson, J.G.

832 (2014) BAMMtools: an R package for the analysis of evolutionary dynamics on

833 phylogenetic trees. *Methods in Ecology and Evolution*, **5**, 701-707.

834 Rabosky, D.L., Chang, J., Title, P.O., Cowman, P.F., Sallan, L., Friedman, M., Kaschner, K.,

835 Garilao, C., Near, T.J., Coll, M., Alfaro, M.E. (2018). An inverse latitudinal gradient

836 in speciation rate for marine fish. *Nature*, **559**, 392-395.

837 Ricklefs, R.E. (2014) Reconciling diversification: random pulse models of speciation and

838 extinction. *American Naturalist* **184**, 268-276.

839 Ranwez, V., Harispe, S., Delsuc, F. & Douzery, E.J.P. (2011) MACSE: Multiple Alignment of

840 Coding SEquences accounting for frameshifts and stop codons. *Plos ONE*, **6**

841 Revell, L.J. (2012) phytools: an R package for phylogenetic comparative biology (and other

- 842 things). *Methods in Ecology and Evolution*, **3**, 217-223.
- 843 Rohde, K. (1992) Latitudinal gradients in species diversity: the search for the primary cause.
844 *Oikos*, 514-527.
- 845 Rolland, J., Condamine, F.L., Jiguet, F. & Morlon, H. (2014) Faster speciation and reduced
846 extinction in the tropics contribute to the mammalian latitudinal diversity gradient.
847 *PLoS Biology*, **12**, e1001775.
- 848 Santini, L., González-Suárez, M., Rondinini, C., Di Marco, M. (2017) Shifting baseline in
849 macroecology? Unravelling the influence of human impact on mammalian body mass.
850 *Diversity and Distributions*, **23**, 640-659.
- 851 Sarnat, E.M. & Moreau, C.S. (2011) Biogeography and morphological evolution in a Pacific
852 island ant radiation. *Molecular Ecology*, **20**, 114-130.
- 853 Siqueira, A.C., Oliveira-Santos, L.G.R., Cowman, P.F., Floeter, S.R., Algar, A. (2016)
854 Evolutionary processes underlying latitudinal differences in reef fish diversity. *Global
855 Ecology and Biogeography*, **25**, 1466-1476.
- 856 Stamatakis, A. (2014) RAxML version 8: a tool for phylogenetic analysis and post-analysis
857 of large phylogenies. *Bioinformatics*, **30**, 1312-1313.
- 858 Stephens, P.R. & Wiens, J.J. (2003) Explaining species richness from continents to
859 communities: The time-for-speciation effect in emydid turtles. *American Naturalist*,
860 **161**, 112-128.
- 861 Turvey, S.T. & Fritz, S.A. (2011) The ghosts of mammals past: biological and geographical
862 patterns of global mammalian extinction across the Holocene. *Philosophical
863 Transactions of the Royal Society of London B: Biological Sciences*, **366**, 2564-76.
- 864 Ward, P.S., Brady, S.G., Fisher, B.L. & Schultz, T.R. (2015) The evolution of myrmicine ants:
865 phylogeny and biogeography of a hyperdiverse ant clade (Hymenoptera: Formicidae).
866 *Systematic Entomology*, **40**, 61-81.
- 867 Weir, J.T. & Schluter, D. (2007) The latitudinal gradient in recent speciation and extinction
868 rates of birds and mammals. *Science*, **315**, 1574-1576.
- 869 Wiens, J.J. & Donoghue, M.J. (2004) Historical biogeography, ecology and species richness.
870 *Trends in Ecology & Evolution*, **19**, 639-644.
- 871 Wiens, J.J. & Graham, C.H. (2005) Niche conservatism: Integrating evolution, ecology, and
872 conservation biology. *Annual Review of Ecology Evolution and Systematics*, **36**, 519-
873 539.
- 874 Willig, M.R., Kaufman, D.M. & Stevens, R.D. (2003) Latitudinal gradients of biodiversity:
875 Pattern, process, scale, and synthesis. *Annual Review of Ecology Evolution and*

876 Systematics, **34**, 273-309.

877

878 **DATA ACCESSIBILITY**

879 Molecular sequences have been deposited to GenBank (see Table S1 for accession numbers).

880 We have also provided the alignment, BEAST xml file, and geographic dataset in a

881 supplemental data archive (Dryad XXX). The GABI dataset can be accessed on the

882 interactive website antmaps.org.

883

884 **Acknowledgements:** This work was supported by NSF (DEB-1145989 to EPE and LLK), by
885 subsidy funding to OIST, and by a Japan Society for the Promotion of Science Kakenhi
886 (17K15180) to EPE. We thank P.S. Ward and B.L. Fisher for sharing specimens and for all
887 the data contributors to the GABI project.

888

889 **Biosketch:** The research team is interested in the ecology and evolution of biodiversity,
890 especially insects.

891

892 **Supplementary Information**

893

894 **Appendix 1:** Calculation of sampling completeness across geography and clade

895

896 **Appendix 2:** GeoSSE methods, analysis, and discussion

897

898 **Figure S1:** An expanded version of the phylogeny depicted in Figure 2, with readable tips
899 and node supports.

900

901 **Table S1:** List of specimens and GenBank accession numbers for the taxa used in this study

902

903

904

905 **Figure Legends**

906

907 **Figure 1:** Global patterns of Pheidole species richness plotted by a) geographic region and b)
908 5-degree latitudinal band for 1138 described species/subspecies and 361 morphospecies. For
909 comparison, latitudinal distribution of 13771 ant species excluding Pheidole are also

910 depicted. Latitudinal richness is expressed as fraction of total richness (1499 for Pheidole,
911 13771 for all other ants).

912

913 **Figure 2:** Diversification rate dynamics inferred with BAMM from a phylogeny of 449
914 Pheidole species. a) Median diversification rates through time of the major Pheidole clades.
915 The New World median excludes the two early branching species (*P. rhea* and *P. fimbriata*)
916 that fall outside the initial acceleration of Pheidole diversification. b) The maximum clade
917 credibility phylogeny colored with inferred net diversification rate. c) Latitudinal extent of all
918 449 taxa included in the tree. A high-resolution version with taxon names visible is presented
919 in Figure S1. d) Probable locations of diversification rate shifts. Here, branch length is
920 proportional to probability of a shift.

921

922

923 **Figure 3:** Net diversification rate inferred with BAMM as a function of latitude.
924 Diversification rate of each Pheidole species (present day) inferred with BAMM using the
925 “M” assumption of sampling completeness per species a) as a function of latitudinal midpoint
926 and b) tropicality index, which varies from -1 for a species with a range located completely
927 outside the tropics to 1 for a species confined to the tropics. c) Spearman correlations (black
928 dots) for net diversification and either absolute midpoint latitude (left) or tropicality (right),
929 where the grey boxes reflect 95% null distribution generated with STRAPP. L, M, H, reflect
930 different assumptions about unsampled species (low, medium, high estimates of total
931 numbers of Pheidole), while M* are 10 trees where temperate species have been culled to
932 account for possible sampling bias (see methods).

933

934 **Figure 4:** Evolution of latitudinal affinity in Pheidole. a) Branch-wise probability of
935 ancestral tropical state inferred from stochastic character mapping. b-c) Histograms of
936 latitudinal richness differences between tropics and extratropics simulated with stochastic
937 character mapping on the empirical phylogeny assuming a tropical ancestor and the inferred
938 degree of niche conservation using symmetric (b) or asymmetric (c) models of character
939 evolution. The vertical dashed line is the empirical richness fraction.

940

941

942

943

944
 945
 946
 947

Table 1: Summary of delta AICc from the BiSSE and HiSSE trait-dependent models, and the two null models, CID-2 and CID-4. CID-2 is similar in model complexity to the BiSSE model, while CID-4 is similar in model complexity to the HiSSE model. The models were run with different parameter constraints listed below. The L, M, H, refer to the low, medium, and high estimates of missing taxa. M* includes a correction for possible oversampling with latitude. The AICc minimizing model for each analysis is highlighted in bold.

Model	Description/constraint	Global Pheidole (Δ AICc)			New World Pheidole (Δ AICc)			
		L	M	H	L	M	H	M*
BiSSE	Div. rates and transition rates equal across latitudes	69.9	67.4	69.6	18.3	23.2	27.8	23.2
BiSSE	Div. rates equal, transition rates vary with latitude	69.4	66.9	69.2	19.4	24.2	28.9	22.3
BiSSE	Div rates vary, transition rates equal with latitude	69.9	67.4	69.6	18.3	23.2	27.8	23.2
BiSSE	Div. rates and transition rates vary with latitude (full BiSSE model)	73.5	71.1	73.3	11.6	16.1	18.9	23.2
CID-2 null	2 hidden states, 1 transition parameter	33.9	21.9	17.3	0.5	2.8	5.7	2.9
CID-2 null	2 hidden states, 3 transition parameters	21.2	20.1	19.4	2.4	5.3	8.6	4.5
HiSSE	Div rates vary with latitude and two hidden states, 1 transition parameter	36.1	21.1	16.5	0.9	0.9	0.3	8.6
HiSSE	Div rates vary with latitude and two hidden states, 3 transition parameters	22.5	28.0	27.7	0.2	2.0	2.3	9.5
CID-4 null	Div rates vary with four hidden states, 1 transition parameter	22.5	11.1	4.6	1.6	0.0	0.0	0.0
CID-4 null	Div. rates vary with four hidden states, 3 transition parameters	0.0	0.0	0.0	0.0	1.1	0.4	5.7

948

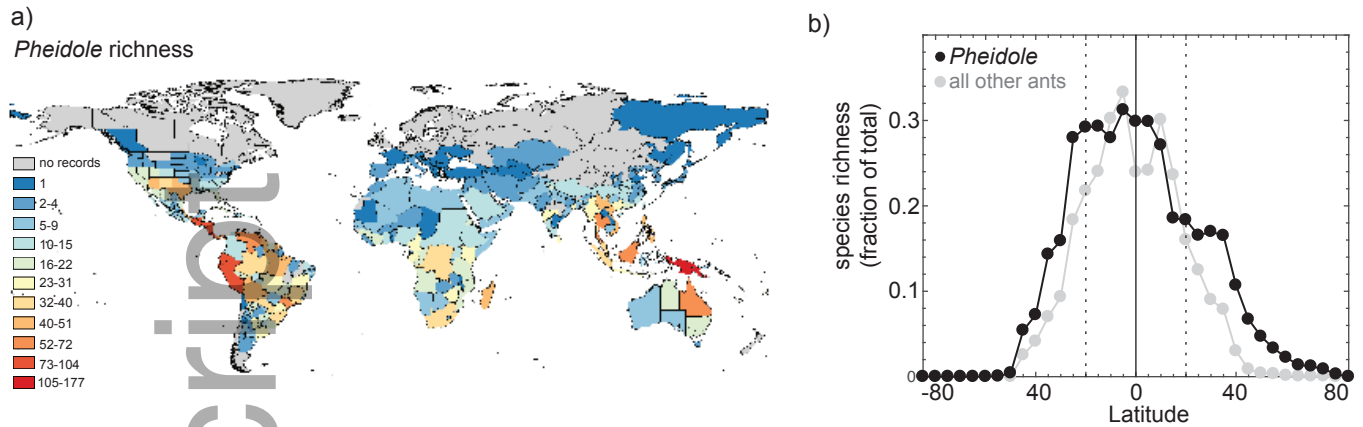


Figure 1 : Global patterns of *Pheidole* species richness plotted by a) geographic region and b) 5-degree latitudinal band for 1138 described species/subspecies and 361 morphospecies. For comparison, latitudinal distribution of 13771 ant species excluding *Pheidole* are also depicted. Latitudinal richness is expressed as fraction of total richness (1499 for *Pheidole*, 13,771 for all other ants).

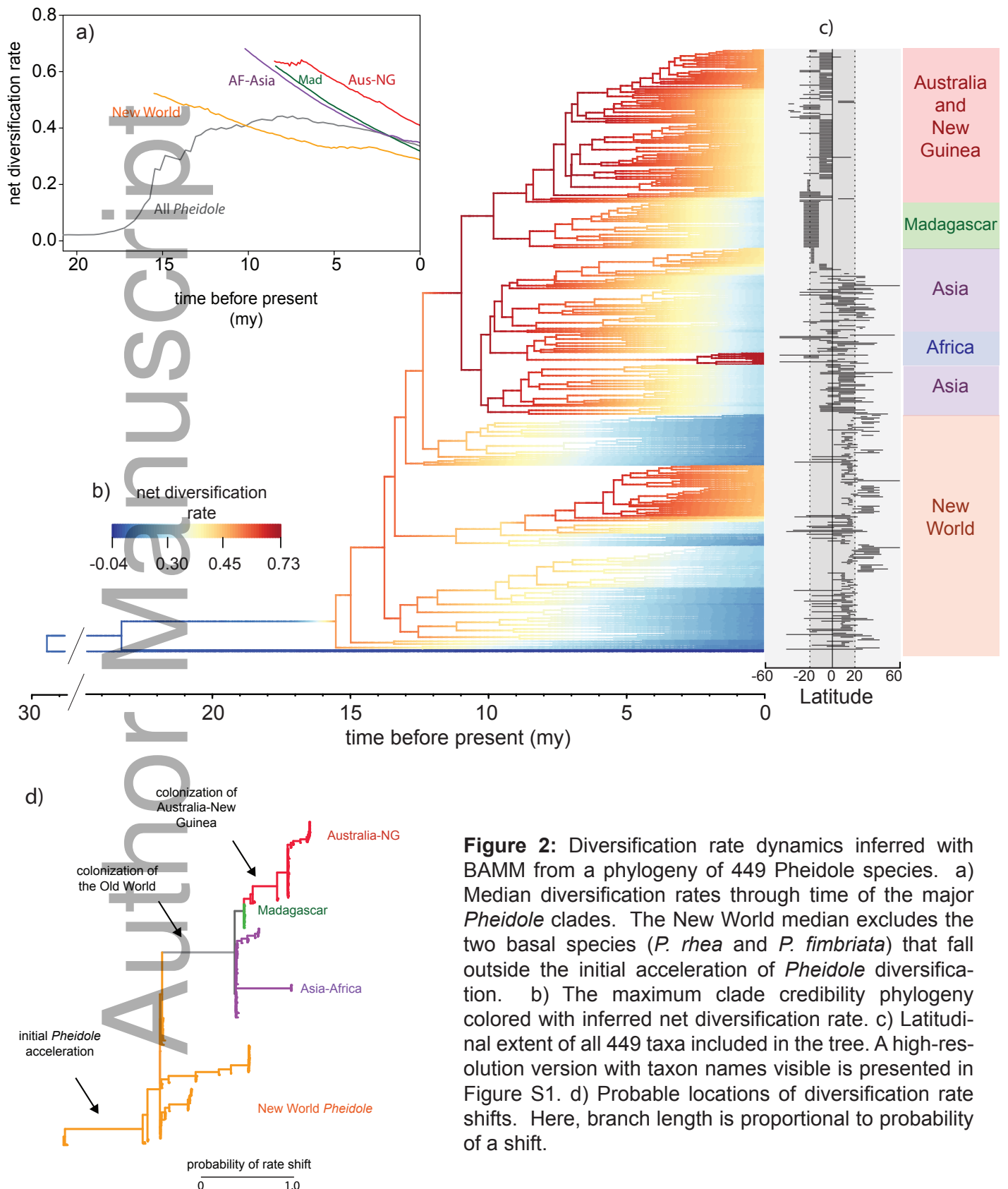


Figure 2: Diversification rate dynamics inferred with BAMM from a phylogeny of 449 *Pheidole* species. a) Median diversification rates through time of the major *Pheidole* clades. The New World median excludes the two basal species (*P. rhea* and *P. fimbriata*) that fall outside the initial acceleration of *Pheidole* diversification. b) The maximum clade credibility phylogeny colored with inferred net diversification rate. c) Latitudinal extent of all 449 taxa included in the tree. A high-resolution version with taxon names visible is presented in Figure S1. d) Probable locations of diversification rate shifts. Here, branch length is proportional to probability of a shift.

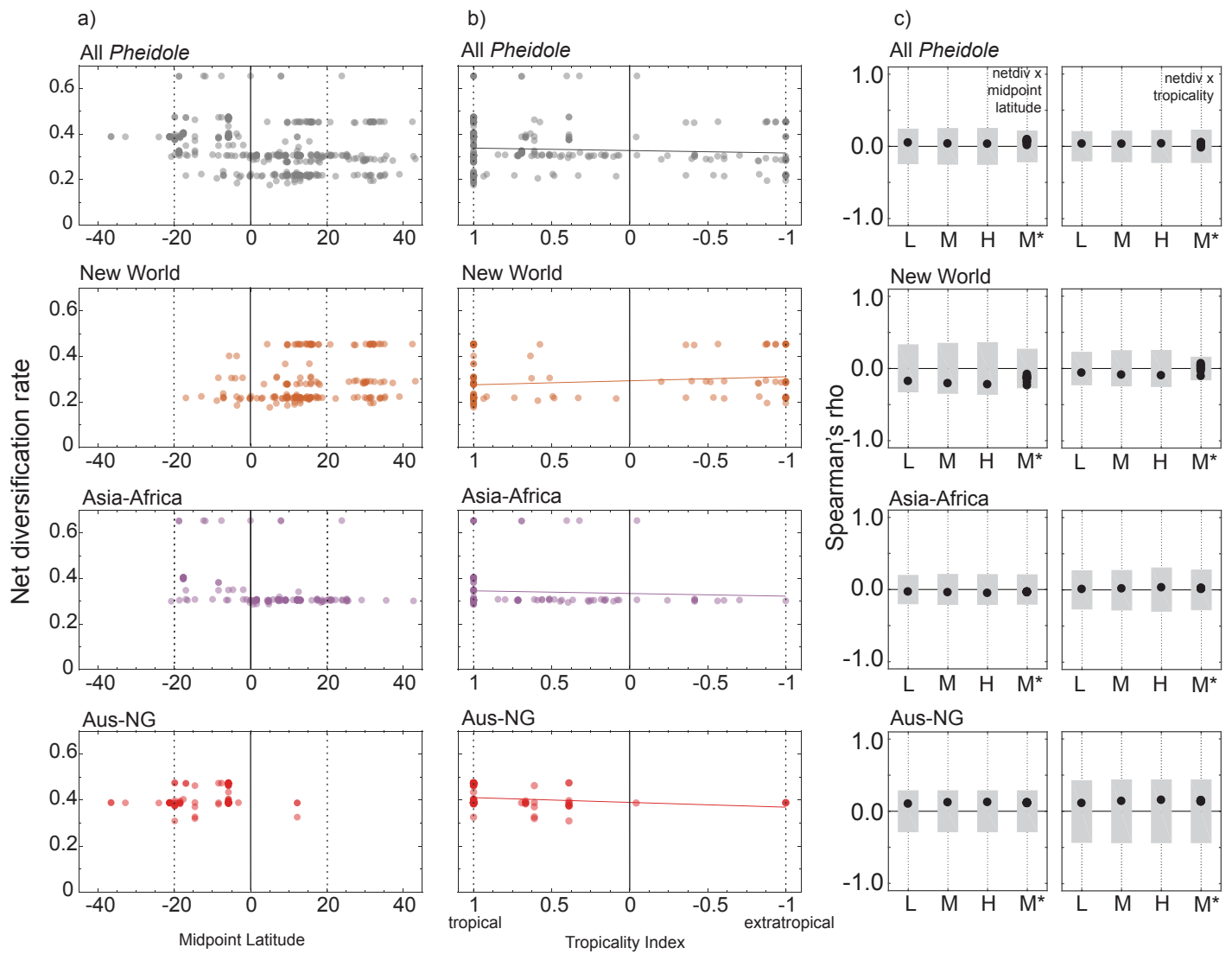


Figure 3: Net diversification rate inferred with BAMM as a function of latitude. Diversification rate of each *Pheidole* species (present day) inferred with BAMM using the “M” assumption of sampling completeness per species a) as a function of latitudinal midpoint and b) tropicity index, which varies from -1 for a species with a range located completely outside the tropics to 1 for a species confined to the tropics. c) Spearman correlations (black dots) for net diversification and either absolute midpoint latitude (left) or tropicity (right), where the grey boxes reflect 95% null distribution generated with STRAPP. L, M, H, reflect different assumptions about unsampled species (low, medium, high estimates of total numbers of *Pheidole*), while M* are 10 trees where temperate species have been culled to account for possible sampling bias (see methods).

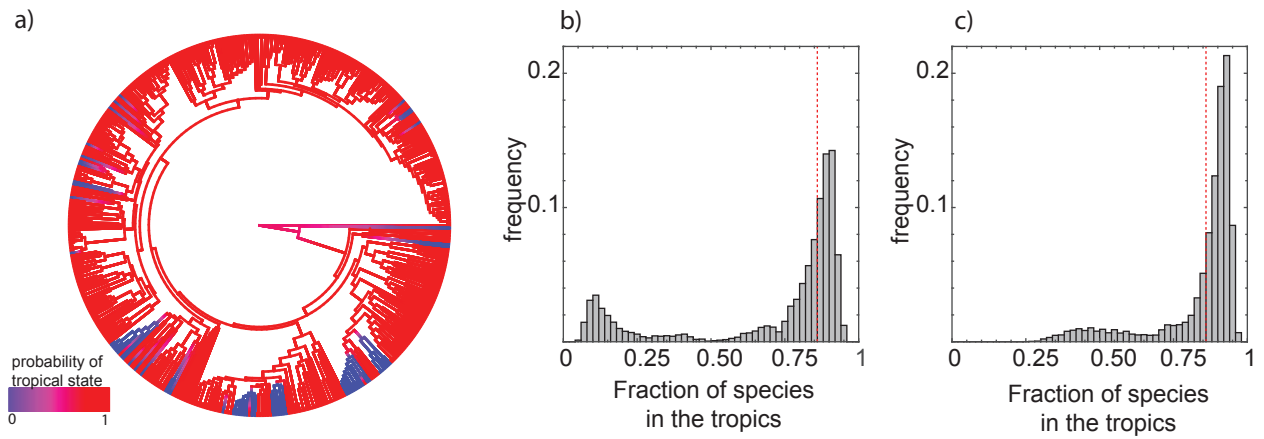


Figure 4 : Evolution of latitudinal affinity in *Pheidole*. a) Branch-wise probability of ancestral tropical state inferred from stochastic character mapping. b-c) Histograms of latitudinal richness differences between tropics and extratropics simulated with stochastic character mapping on the empirical phylogeny assuming a tropical ancestor and the inferred degree of niche conservation using symmetric (b) or asymmetric (c) models of character evolution. The vertical dashed line is the empirical richness fraction.